Symmetry-preserving nudging: theory and application to a shallow water model

Didier Auroux, Silvère Bonnabel

INRIA

INSTITUT NATIONAL DE RECHERCHE EN INFORMATIQUE ET EN AUTOMATIQUE

Symmetry-preserving nudging: theory and application to a shallow water model

Didier Auroux — Silvère Bonnabel

N° 6677

Octobre 2008

Thème NUM

ISSN 0249-6399 ISRN INRIA/RR--6677--FR+ENG

INSTITUT NATIONAL
DE RECHERCHE
EN INFORMATIQUE
ET EN AUTOMATIQUE

INRIA

centre de recherche
GRENOBLE - RHÔNE-ALPES

Symmetry-preserving nudging: theory and application to a shallow water model

Didier Auroux*† , Silvère Bonnabel‡

Thème NUM — Systèmes numériques
Équipe-Projet MOISE

Rapport de recherche n° 6677 — Octobre 2008 — 25 pages

Abstract: One of the important topics in oceanography is the prediction of ocean circulation. The goal of data assimilation is to combine the mathematical information provided by the modeling of ocean dynamics with observations of the ocean circulation, e.g. measurements of the sea surface height (SSH). In this paper, we focus on a particular class of extended Kalman filters as a data assimilation method: nudging techniques, in which a corrective feedback term is added to the model equations. We consider here a standard shallow water model, and we define an innovation term that takes into account the measurements and respects the symmetries of the physical model. We prove the convergence of the estimation error to zero on a linear approximation of the system. It boils down to estimating the fluid velocity in a water-tank system using only SSH measurements. The observer is very robust to noise and easy to tune. The general nonlinear case is illustrated by numerical experiments, and the results are compared with the standard nudging techniques.

Key-words: Nudging, observer, symmetries, shallow water model, partial differential equation, estimation, data assimilation.

* Institut de Mathématiques de Toulouse, Université Paul Sabatier Toulouse 3, 31062 Toulouse cedex 9, France (auroux@math.univ-toulouse.fr)
† INRIA Grenoble Rhône-Alpes, équipe-projet MOISE, France
‡ University of Liege, Belgium (bonnabel@montefiore.ulg.ac.be)

Centre de recherche INRIA Grenoble – Rhône-Alpes
655, avenue de l'Europe, 38334 Montbonnot Saint Ismier
Téléphone : +33 4 76 61 52 00 — Télécopie +33 4 76 61 52 52

Observateurs et nudging invariants: théorie et application à un modèle shallow-water

Résumé : La prévision de la circulation des océans est un enjeu crucial en océanographie. L'assimilation de données consiste à coupler l'information mathématique provenant de la modélisation de la dynamique des océans avec les observations de la circulation océanique, par exemple des mesures de hauteur d'eau (SSH). Dans cet article, nous étudions une méthode particulière de la classe des filtres de Kalman étendus: le nudging, consistant à ajouter un terme de rappel aux données dans les équations du modèle. On considère ici un modèle shallow-water, et nous définissons un terme de rappel qui prend en compte les données et qui respecte les symétries du modèle physique. Nous démontrons la convergence de l'erreur d'estimation vers 0 sur une approximation linéaire du système. Cela prouve la possibilité de reconstruire l'état complet du système à partir de données SSH uniquement. L'observateur ainsi construit est très robuste au bruit et facile à régler. Le cas général (non linéaire) est illustré par plusieurs expériences numériques, et les résultats sont comparés à ceux obtenus à l'aide du nudging standard.

Mots-clés : Nudging, observateur, symétries, modèle shallow water, équations aux dérivées partielles, estimation, assimilation de données.

1 Introduction

Data assimilation consists in estimating the state of a system combining two different sources of information via numerical methods: models, and observations. There is an increasing need for such methods in physical oceanography, as the monitoring of the ocean provides crucial information about climate changes [21], and the models, although very complex, need to be combined with the observations of ever increasing quality. Notably, the amount of data available in oceanography has drastically increased in the last years with the use of satellites.

This paper deals with data assimilation, focusing on a particular technique: nudging. The standard nudging algorithm consists in applying a Newtonian recall of the state value towards its direct observation [10]. From another point of view, the principle of nudging is to use observers of the Luenberger, or extended Kalman filter type for data assimilation [16, 12]. The model appears then as a weak constraint, and the nudging term forces the state variables to fit as well as possible the observations. This forcing term in the model dynamics has a tunable coefficient that represents the relaxation time scale. This coefficient is usually chosen by numerical experimentation so as to keep the nudging terms small in comparison with the state equations, and large enough to force the model to fit the observations. The nudging term can also be seen as a penalty term, which penalizes the system if the model is too far from the observations. The nudging method, or more generally observers, is a flexible assimilation technique, computationally much more economical than variational data assimilation methods [24, 15].

Observers of the Kalman filter type are designed to provide, for each time step, the optimal estimate (i.e. of minimal error variance) of the system state, by using only the previous estimates of the state and the last observations [12, 9]. These filters alternate propagation steps (with the physical model) and correction steps (using the observations) of the state and of its error statistics. In the case of a non-linear physical model the extended Kalman filter only yields an approximation of the optimal estimate. As the oceanographic models have become very complex in the recent years, the high computing cost of the extended Kalman filter can be prohibitive for data assimilation [21]. The nudging techniques take advantage of the form of the Kalman filter, alternating propagation and correction steps but the gain matrices (or coefficients) are often chosen to be constant, and their expression requires very few (or no) calculations [10, 23].

Most Kalman-type filters, or Luenberger observers [16] do not take into account the symmetries of the model. But the symmetries often contain useful geometrical information on the model that can help for the design and improve the performances. Indeed, there has been recent work on observer design and symmetries for engineering problems when the model is of finite dimension and when there is a Lie group acting on the state space [2, 1, 17, 7, 6]. Symmetries provide a helpful guide to design correction terms based on the very structure of the physical system. The only difference between the observer and model equations comes from the correction term. When this term is bound to preserve symmetries, the observer is called "invariant", or "symmetry-preserving". The result is that the estimations do not depend on arbitrary choices of units or coordinates, and the estimates share common physical properties with the system variables (in the examples given in [7], estimated concentrations are automati-

cally positive, estimated rotation matrices automatically belong to $SO(3)$). In some cases, the error system even presents very nice properties (autonomous error equation in [6]).

This paper is an extension to the infinite-dimensional case of the recent ideas on observer design and symmetries for systems described by ordinary differential equations (ODE) [7], in the particular context of nudging for data assimilation in oceanography. The problem considered is the following: the ocean is described by a simplified shallow-water model. The sea surface height (SSH) is measured (with noise) everywhere by satellites. The goal is to estimate the height, and the (not measured) marine currents. The model considered is invariant by rotation and translation ($SE(2)$-invariance). In the case of problems described by infinite dimensional partial differential equations (PDE), the design of observers based on the symmetries of the physical system is new to the authors' knowledge.

The main contribution of this paper is to derive a large class of observers based on the $SE(2)$-invariance for this estimation problem. At first we are only interested in the structure of the observers, and we do not check the validity of the estimation. Then we pick a particular observer in this class. It has several remarkable properties as the design is based on physical considerations. The correction term does not depend on any non-trivial choice of coordinates. Moreover, it is made of a smoothing term which ensures remarkable robustness to white noise. The correction term consists in fact in a convolution of the estimation error with a smooth isotropic kernel. The idea to derive systematical smoothing terms based on physical symmetries is standard in image processing, and was initiated by [3]. One of the simplest method consists in a convolution with a smooth rotation-invariant kernel (isotropic diffusion based on the heat equation). But in this paper we combine the smoothing term with a dynamical model to provide an estimation of physical quantities which are not directly measured, i.e. we build an observer. The second main contribution of the paper is to yield a proof of convergence of the estimation error to zero on a simplified shallow water model. The proof shows how to handle the convolution term via a Fourier analysis. In fact we solve the following estimation problem: predicting the velocity in a water-tank using (very) noisy continuous measurements of the height everywhere at any time. Thus this paper can be viewed as a counterpart in the observer field of the work on the controllability of a water tank, which was raised by [8]. Finally, a noticeable fact is that the observer depends on a small number of parameters, as the structure of the observer is imposed by the structure of the system. All these parameters admit a physical interpretation. So the observer gains are easy to tune, and the corresponding computing cost is quite low, contrarily to the extended Kalman filter. This property is in fact characteristic of symmetry-preserving observers [7]. The performances of the observer and the low computational cost have been numerically tested.

The paper is organized as follows. In Section 2 we consider a bi-dimensional shallow water model, often used in geophysics for ocean or fluid flow modeling. We define a class of invariant observers in the case of SSH observations. Then, we prove the convergence of the estimation error to zero on the first-order approximation of this system. Indeed we assume that the fluid motion is described by linearized wave equations under shallow-water approximations. In Section 3, we report the results of extensive numerical simulations on both the linearized (and simplified) and nonlinear shallow water models. We show the interest of invariant observers in these cases. These results are also compared with the

standard nudging technique, which can be seen as a particular situation of our symmetry-preserving observers. We also show their remarkable robustness to gaussian white noise on the observations. Finally, some conclusions and perspectives are given in Section 4.

2 Nudging and symmetries

In this section we consider a simplified oceanic model. The state of the ocean is the SSH, and the horizontal speed of the marine currents. The choice of the orientation and the origin of the frame of $\mathbb{R}^2$ used to express the horizontal coordinates $(x, y) \in \mathbb{R}^2$ is arbitrary: the physical problem is invariant by rotation and translation. Indeed from a mathematical point of view the Laplace operator Δ is invariant by rotation and translation. The first term of any observer for this problem is automatically invariant by rotation and translation, as it is a copy of the equations of the physical system. There is no reason why the correction term should depend on any non-trivial choice of the orientation and origin of the frame. It would yield correction terms giving more importance to the values of the height measured in some arbitrary direction of $\mathbb{R}^2$. In the general case, without additional information on the model, it seems perfectly logical indeed to correct the observer isotropically. This constraint suggests interesting correction terms.

2.1 Shallow water model

The shallow water model (or Saint-Venant's equations) is a basic model, representing quite well the temporal evolution of geophysical flows. This model is usually considered for simple numerical experiments in oceanography, meteorology or hydrology [19]. These equations are derived from a vertical integration of the three-dimensional fields, assuming the hydrostatic approximation, i.e. neglecting the vertical acceleration. We consider here the shallow water model of Jiang et al [11]. For deeper water, this model can be adapted into a multilayer model, each layer being described by a shallow water model, with some additional terms modeling stress and friction due to the other layers.

The fluid is made of one layer of constant density ρ and with varying thickness (or height) $h(x, y, t)$, covering a deeper layer of density $\rho+\Delta\rho$. The domain is rectangular: $0 \leq x \leq L$ and $0 \leq y \leq L$, where x and y are the cartesian coordinates corresponding to East and North respectively. Let ∇ be the corresponding gradient operator:

$$\nabla = \left(\frac{\partial}{\partial x}, \frac{\partial}{\partial y}\right)^T.$$

The equations write:

$$\frac{\partial(hv)}{\partial t} + (\nabla \cdot (hv) + (hv) \cdot \nabla)v = -g'h\nabla h - \mathbf{k} \times f(hv) + (\alpha_A A\nabla^2 - R)(hv) + \alpha_{tau}\tilde{\tau}\mathbf{i}/\rho, \tag{1}$$

$$\frac{\partial h}{\partial t} = -\nabla \cdot (hv), \tag{2}$$

where $hv = h(v_x\mathbf{i}+v_y\mathbf{j})$ is the horizontal transport, with $\mathbf{i}$ and $\mathbf{j}$ pointing towards East and North respectively, $f = f_0 + \beta(y - 0.5D)$ is the Coriolis parameter (in

the β-plane approximation), $\mathbf{k}$ is the upward unit vector, and g' is the reduced gravity. The ocean is driven by a zonal wind stress $\tilde{\tau}\mathbf{i}$ modeled as a body force, and $\tilde{\tau}$ is known. Finally, R and A represent friction and lateral viscosity.

We assume that the physical system is observed by several satellites that provide measurements of the SSH $h(x,y,t)$ for all x,y,t. Within the framework of data assimilation for geophysical fluids, the goal is to estimate all the state variables $v(x,y)$ and $h(x,y)$ (velocity of the marine streams, and SSH respectively) at any point $(x,y) \in [0,L]^2$ of the domain. We finally consider that all the other parameters are known. Note that the state space is of infinite dimension.

2.2 Model symmetries

The unit vectors $\mathbf{i}$ and $\mathbf{j}$ are pointing East and North respectively. This choice is arbitrary, and the equations of fluid mechanics do not depend neither on the orientation nor on the origin of the frame in which the coordinates are expressed: they are invariant under the action of $SE(2)$, the *Special Euclidean* group of isometries of the plane $\mathbb{R}^2$. Let us prove this invariance. Let $R_\theta = \begin{pmatrix} \cos\theta & -\sin\theta \\ \sin\theta & \cos\theta \end{pmatrix}$ be a horizontal rotation of angle θ. Let $(x_0,y_0) \in \mathbb{R}^2$ be the origin of the new frame. Let (X,Y) be the coordinates associated to the new frame $R_{-\theta}(\mathbf{i},\mathbf{j}) - (x_0,y_0)$. In this new frame, the variables read

$$
\begin{aligned}
(X,Y) &= R_\theta(x,y) + (x_0,y_0), && (3)\\
H(X,Y) &= h(x,y), && (4)\\
V(X,Y) &= R_\theta v(x,y). && (5)
\end{aligned}
$$

and $(\frac{\partial}{\partial X}, \frac{\partial}{\partial Y}) = R_\theta(\frac{\partial}{\partial x}, \frac{\partial}{\partial y})$ which implies $\nabla H(X,Y) = R_\theta \nabla h(x,y)$. The equations in the new coordinates read the same with the notations $\mathbf{K} = \mathbf{k}$ and $\mathbf{I} = R_\theta \mathbf{i}$:

$$
\begin{aligned}
\frac{\partial(HV)}{\partial t} + (\nabla\cdot(HV) + (HV)\cdot\nabla)V &= -g'H\nabla H - \mathbf{K}\times f(HV) && (6)\\
&\quad +(\alpha_A A\nabla^2 - R)(HV) + \alpha_{tau}\tilde{\tau}\mathbf{I}/\rho,\\
\frac{\partial H}{\partial t} &= -\nabla\cdot(HV). && (7)
\end{aligned}
$$

The Laplace and divergence operators are unchanged by the transformation as they are invariant by rotation (although they are usually written in fixed coordinates, their value do not depend on the orientation of the chosen frame). Note that the square domain $D = [0,L]^2 \subset \mathbb{R}^2$ has to be replaced by the square $(R_\theta D + (x_0,y_0)) \subset \mathbb{R}^2$.

2.3 Symmetry-preserving nudging

An observer for the system (1)-(2) (nudging estimator) systematically writes :

$$
\begin{aligned}
\frac{\partial(\hat{h}\hat{v})}{\partial t} + (\nabla\cdot(\hat{h}\hat{v}) + (\hat{h}\hat{v})\cdot\nabla)\hat{v} &= -g'\hat{h}\nabla\hat{h} - \mathbf{k}\times f(\hat{h}\hat{v}) + (\alpha_A A\nabla^2 - R)(\hat{h}\hat{v})\\
&\quad +\alpha_{tau}\tilde{\tau}\mathbf{i}/\rho + F_v(h,\hat{v},\hat{h}), && (8)\\
\frac{\partial\hat{h}}{\partial t} &= -\nabla\cdot(\hat{h}\hat{v}) + F_h(h,\hat{v},\hat{h}), && (9)
\end{aligned}
$$

with $\hat{h} = h$ on the boudary of the domain, and where the correction terms vanish when the estimated height $\hat{h}$ is equal to the observed height h:

$$F_v(h, \hat{v}, h) = 0, \quad F_h(h, \hat{v}, h) = 0.$$

No additionnal condition is required on F_v and F_h at this stage. They are functionals, and they can be for instance differential or integral operators of the space variables. The next step is to consider correction terms that respect the underlying physics of the system in the sense that they are invariant under the action of $SE(2)$. Indeed why the quality of the estimation should depend upon the choice of orientation and origin of the frame when the physical system under consideration does not at all? Let us search the correction terms in the large class of $SE(2)$-invariant differential and integral terms.

Invariant correction terms

We look for three types of invariant correction terms: scalar, differential, and integral. Let us first focus on the former two. Note that F_v is a vector and F_h a scalar. To find F_h, we use the standard result (see e.g. [22]), which states that any $SE(2)$-invariant scalar differential operator writes $Q(\Delta)$, where Q is a polynomial and Δ is the Laplacian.

In our case, the coefficients of this polynomial can be invariant functions of the estimated state $(\hat{h}, \hat{v})$ and measurement h. Note that $\hat{v}$ is the unique vectorial function amongst these variables. The scalar variables h and $\hat{h}$ are $SE(2)$-invariant when transformed accordingly to (4). Thus any scalar invariant function of $(h, \hat{h}, \hat{v})$ must depend on $\hat{v}$ only via an invariant function of $\hat{v}$, typically $|\hat{v}|^2$. Indeed, using polar coordinates it is clear that it is the unique quantity that does not depend on the angle between $\hat{v}$ and the (arbitrary) axis of the frame (see e.g. [18, 7] for the construction of a complete set of scalar invariants). But since differential terms are allowed, and the gradient ∇ is a vectorial differential operator which rotates under the action of $SE(2)$, one can get some rotation-invariant scalar terms from the scalar product between the gradient of invariant quantities, and the only vectorial function at our disposal $\hat{v}$. Eventually, we get a complete family of scalar terms F_h :

$$F_h = Q_1(\Delta, h, |\hat{v}|^2, \hat{h} - h) + \nabla \left(Q_2(\Delta, h, |\hat{v}|^2, \hat{h} - h) \right) \cdot \hat{v} + f_h, \qquad (10)$$

where Q_1 and Q_2 are scalar polynomials in Δ, and f_h is an integral term defined below. More precisely, for $i = 1, 2$, we have

$$Q_i(\Delta, h, |\hat{v}|^2, \hat{h} - h) = \sum_{k=0}^{N} a_k^i(h, |\hat{v}|^2, \hat{h} - h)\ \Delta^k \left(b_k^i(h, |\hat{v}|^2, \hat{h} - h) \right), \qquad (11)$$

where a_k^i and b_k^i are smooth scalar functions such that

$$a_k^i(h, |\hat{v}|^2, 0) = b_k^i(h, |\hat{v}|^2, 0) = 0. \qquad (12)$$

For the vectorial correction term F_v, we use the vectorial counterpart:

$$F_v = P_1(\Delta, h, |\hat{v}|^2, \hat{h} - h)\ \hat{v} + \nabla \left(P_2(\Delta, h, |\hat{v}|^2, \hat{h} - h) \right) + f_v, \qquad (13)$$

where P_1 and P_2 are polynomials in Δ, like Q_1 and Q_2.

Let us now find the integral terms f_h and f_v that are invariant by rotation and translation. They can be expressed as a convolution between the previous invariant differential terms and a two-dimensional kernel $\psi(\xi,\zeta)$. The previous terms being invariant by rotation, the value of the kernel should not depend on any particular direction, and so ψ must be a function of the invariant $\xi^2+\zeta^2$ (isotropic gain). So if we let ϕ_v and ϕ_h be two real-valued kernels, the integral correction terms write:

$$\begin{aligned} f_v(x,y,t) &= \iint \phi_v(\xi^2+\zeta^2)\Big[R_1(\Delta,h,|\hat{v}|^2,\hat{h}-h)\hat{v} \\ &\quad + \nabla\Big(R_2(\Delta,h,|\hat{v}|^2,\hat{h}-h)\Big)\Big]_{(x-\xi,y-\zeta,t)}\, d\xi d\zeta, \qquad (14) \\ f_h(x,y,t) &= \iint \phi_h(\xi^2+\zeta^2)\Big[S_1(\Delta,h,|\hat{v}|^2,\hat{h}-h) \\ &\quad + \nabla\Big(S_2(\Delta,h,|\hat{v}|^2,\hat{h}-h)\Big)\cdot\hat{v}\Big]_{(x-\xi,y-\zeta,t)}\, d\xi d\zeta, \qquad (15) \end{aligned}$$

where the polynomials R_i and S_i are defined like the Q_i's.

The support of ϕ_v (resp. ϕ_h) is a subset of $\mathbb{R}$. Its characteristic size defines a zone in which it is significant to correct the estimation with the measurements. The radial term $\xi^2+\zeta^2$ makes the observer independent of any arbitrary choice of orientation (invariance by rotation), and the use of a convolution makes the observer independent of the origin of the frame (invariance by translation). The integral formulation is actually quite general: if ϕ_v and ϕ_h are set equal to Dirac functions, one obtains the differential terms.

Such integral correction terms make the observer robust to noise. Indeed if the kernels are smooth, the correction terms take into account the measurements, but are automatically smooth even if the measurements are not. The high frequencies in the signal are thus efficiently filtered.

2.4 Convergence study on a linearized simplified system

As it seems very difficult to study the convergence on the full non-linear system, we are going to simplify the system (1)-(2) in this section, and then linearize it around the equilibrium position $h=\bar{h}$ and $v=\bar{v}$. In our experiments, the equilibrium is characterized by $\bar{h}$ equal to a constant height, and $\bar{v}=0$. The observer gains are designed on this latter system, and then we prove at the end of this section that they ensure the strong asymptotic convergence of the error.

For reasons of clarity, we first consider a simplified shallow water model (Saint-Venant equations):

$$\begin{aligned} \frac{\partial h}{\partial t} &= -\nabla(hv), \qquad (16) \\ \frac{\partial v}{\partial t} &= -v\nabla v - g\nabla h. \qquad (17) \end{aligned}$$

In order to avoid the amplification of the measurement noise by a differentiation process, only the integral correction terms are kept: one sets $Q_1=Q_2=P_1=P_2=0$, $R_1=S_2=0$, and $R_2=S_1=h-\hat{h}$, and the kernels ϕ_h and ϕ_v are supposed to be smooth functions. Thus the correction terms are smooth, and

one can use the gradient of the output, as it is filtered. The symmetry-preserving observer (8)-(9) for the simplified system (16)-(17) writes:

$$\begin{aligned}\frac{\partial \hat{h}}{\partial t} &= -\nabla(\hat{h}\hat{v}) + \iint \phi_h(\xi^2+\zeta^2)\ (h-\hat{h})_{(x-\xi,y-\zeta,t)}\ d\xi d\zeta \\ &= -\nabla(\hat{h}\hat{v}) + \varphi_h * (h-\hat{h}), \qquad (18)\\ \frac{\partial \hat{v}}{\partial t} &= -\hat{v}\nabla\hat{v} - g\nabla\hat{h} + \iint \phi_v(\xi^2+\zeta^2)\ \nabla(h-\hat{h})_{(x-\xi,y-\zeta,t)}\ d\xi d\zeta \\ &= -\hat{v}\nabla\hat{v} - g\nabla\hat{h} + \varphi_v * \nabla(h-\hat{h}), \qquad (19)\end{aligned}$$

where $\varphi_h(\xi,\zeta) = \phi_h(\xi^2+\zeta^2)$ and $\varphi_v(\xi,\zeta) = \phi_v(\xi^2+\zeta^2)$.

Remark: Note that in the degenerate case where $\phi_h = K_h\delta_0$ and $\phi_v = K_v\delta_0$ (K_h and K_v are positive scalars), we find the standard nudging terms:

$$\begin{aligned}\frac{\partial \hat{h}}{\partial t} &= -\nabla(\hat{h}\hat{v}) + K_h(h-\hat{h}), \qquad (20)\\ \frac{\partial \hat{v}}{\partial t} &= -\hat{v}\nabla\hat{v} - g\nabla\hat{h} + K_v\nabla(h-\hat{h}). \qquad (21)\end{aligned}$$

Using exactly the same simplifications as [20] which considers the control problem and motion planning of system (16)-(17) with boundary control, we study the first order approximation (or linearized approximation) of this system around the steady-state $(h,v) = (\bar{h},0)$, where the equilibrium height $\bar{h}$ is constant. We only consider small velocities $\delta v = v - \bar{v} \ll \sqrt{g\bar{h}}$ and heights $\delta h = h - \bar{h} \ll \bar{h}$. Note that these approximations are consistent with the numerical experiments of Section 3, in which the ratio δv (resp. δh) to $\sqrt{g\bar{h}}$ (resp. $\bar{h}$) is of the order of 10^{-2} to 10^{-3}. The linearized system is

$$\begin{aligned}\frac{\partial(\delta h)}{\partial t} &= -\bar{h}\nabla\delta v, \qquad (22)\\ \frac{\partial(\delta v)}{\partial t} &= -g\nabla\delta h, \qquad (23)\end{aligned}$$

and the estimation errors, $\tilde{h} = \delta\hat{h} - \delta h$ and $\tilde{v} = \delta\hat{v} - \delta v$, are solution of the following linear equations:

$$\begin{aligned}\frac{\partial \tilde{h}}{\partial t} &= -\bar{h}\nabla\tilde{v} - \varphi_h * \tilde{h}, \qquad (24)\\ \frac{\partial \tilde{v}}{\partial t} &= -g\nabla\tilde{h} - \varphi_v * \nabla\tilde{h}. \qquad (25)\end{aligned}$$

Eliminating $\tilde{v}$ and using $\nabla(\varphi_v * \nabla h) = \varphi_v * \Delta h$ yields a modified damped wave equation with external viscous damping:

$$\frac{\partial^2 \tilde{h}}{\partial t^2} = g\bar{h}\Delta\tilde{h} + \bar{h}\,\varphi_v * \Delta\tilde{h} - \varphi_h * \frac{\partial \tilde{h}}{\partial t}. \qquad (26)$$

We now define the kernels φ_v and φ_h. We choose

$$\begin{aligned}\varphi_v(x,y) &= (f(x) * f(x))(f(y) * f(y)), \qquad (27)\\ \varphi_h(x,y) &= (g(x) * g(x))(g(y) * g(y)), \qquad (28)\end{aligned}$$

where f and g are smooth even functions. In order to respect the symmetries, both $\varphi_v(x,y)$ and $\varphi_h(x,y)$ must also be functions of x^2+y^2. The following gaussians respect both conditions:

$$\varphi_v(x,y) = \beta_v \exp(-\alpha_v(x^2+y^2)), \quad (29)$$
$$\varphi_h(x,y) = \beta_h \exp(-\alpha_h(x^2+y^2)), \quad (30)$$

Theorem 1 *If φ_v and φ_h are defined by (29) and (30) respectively with $\beta_v, \beta_h, \alpha_v, \alpha_h > 0$, then the first order approximation of the error system around the equilibrium $(h,v) = (\bar{h}, 0)$ given by (26) is strongly asymptotically convergent. Indeed if we consider the following Hilbert space and norm:*

$$\mathcal{H} = H^1(\Omega) \times L^2(\Omega), \quad \|(u,w)\|_{\mathcal{H}} = \left(\int_\Omega \|\nabla u\|^2 + |w|^2 \right)^{1/2}, \quad (31)$$

then, for every $\tilde{h}$ solution of (26),

$$\lim_{t\to\infty} \left\| \left(\tilde{h}(t), \frac{\partial \tilde{h}}{\partial t}(t) \right) \right\|_{\mathcal{H}} = 0\,. \quad (32)$$

This result proves the strong and asymptotic convergence of the error $\tilde{h}$ towards 0, and then it also gives the same convergence for $\tilde{v}$. We deduce that the observer (18)-(19) tends to the true state when time goes to infinity. Note that although only the height is observed, all variables are corrected, and estimated.

A dimensional analysis can yield a meaningful choice of the gains. The parameters α_v^{-2}, α_h^{-2} are expressed in m. They define the size of the regions of influence of the kernels, i.e. the region around any point in which the measured values of h are used to correct the estimation at the point. These value can be set experimentally using the data from the physical system. Moreover, concerning the tuning of β_v and β_h, one can use the following heuristics. The error system (26) can be approximated by the following system, which corresponds to the case $\alpha = +\infty$:

$$\frac{\partial^2 \tilde{h}}{\partial t^2} + 2\xi_0\omega_0 \frac{\partial \tilde{h}}{\partial t} = (L_0\omega_0)^2 \Delta \tilde{h}. \quad (33)$$

where $L_0^2\omega_0^2 = g\bar{h} + \bar{h}\beta_v$, $2\xi_0\omega_0 = \beta_h$, as long as we impose $L_0^2\omega_0^2 \geq g\bar{h}$. β_v and β_h can be chosen in order to control the characteristic pulsation ω_0, length L_0, and damping coefficient ξ_0 of the approximated error equation (33). These quantities have an obvious physical meaning and can be set accordingly to the characteristics of the physical system under consideration. Such heuristics provide a first reasonable tuning of the gains.

Remark In the following proof, we only use the decomposition of the gain functions given by the general formulation (27) and (28), with some additional assumptions on f and g (see end of section 2.5). Thus, many other kernel functions than those given in (29)-(30) lead to the same convergence result.

2.5 Proof of theorem 1

In this section, inspired by [14], we prove the strong convergence of the error system in the Hilbert space $\mathcal{H}$. Let $\psi_v = g\bar{h}\delta_0 + \bar{h}\varphi_v$. For simplicity reasons, we assume that $L = \pi$. The error equation (26) can be rewritten as a modified wave equation on a square domain with Dirichlet boundary condition:

$$\begin{array}{rcll} \frac{\partial^2}{\partial t^2}u &=& \psi_v * \Delta u - \varphi_h * \frac{\partial}{\partial t}u & \text{in } \mathbb{R}^+ \times \Omega = \mathbb{R}^+ \times [0,\pi]^2, \\ u &=& 0 & \text{on } \mathbb{R}^+ \times \partial\Omega, \\ u(0) &=& u_0, \quad u_t(0) = u_1 & \text{in } \Omega, \end{array} \tag{34}$$

where $u(t,x,y)$ represents the estimation error $\tilde{h}$. The Dirichlet boundary condition comes from the fact that we set $\hat{h} = h$ on the boundary.

We denote by (e_{pq}) the following orthonormal basis of $H_0^1(\Omega)$, composed of eigenfunctions of the unbounded operator Δ:

$$e_{pq} = \frac{2}{\pi}\sin(px)\sin(qy). \tag{35}$$

As f and g are smooth functions ($\mathcal{C}^\infty(\Omega)$ for instance), we can consider their Fourier series expansion. Moreover, as f and g are even functions, their Fourier coefficients are real. If we denote by $(\hat{f}_p)$ and $(\hat{g}_p)$ the Fourier coefficients of f and g respectively, then the Fourier coefficients of ψ_v are $g\bar{h} + \bar{h}\hat{f}_p^2\hat{f}_q^2$. Similarly, the Fourier coefficients of φ_h are $\hat{g}_p^2\hat{g}_q^2$. As all these coefficients are real and positive, we denote them by f_{pq}^2 for ψ_v, and g_{pq}^2 for φ_h. The only assumption that we need on f and g in the following proof is that $\hat{f}_p > 0$ and $\hat{g}_p > 0$, $\forall p$. Note that this condition is satisfied if f and g are defined in a such way that φ_v and φ_h are given by (29)-(30). We now need the following intermediate result:

Lemma 1 *If $u_0 \in H_0^1(\Omega)$ and $u_1 \in L^2(\Omega)$, then equation (34) has a unique solution satisfying*

$$u \in C(\mathbb{R}; H_0^1(\Omega)) \cap C^1(\mathbb{R}; L^2(\Omega)). \tag{36}$$

It is given by the series

$$u(t,x,y) = \frac{2}{\pi}\sum_{1\le p,q} u_{pq}(t)\sin(px)\sin(qy), \tag{37}$$

with either

$$u_{pq}(t) = e^{\frac{-g_{pq}^2}{2}t}(A_{pq}\cos(\omega_{pq}t) + B_{pq}\sin(\omega_{pq}t)), \tag{38}$$

or

$$u_{pq}(t) = e^{\frac{-g_{pq}^2}{2}t}(A_{pq}\cosh(\tilde{\omega}_{pq}t) + B_{pq}\sinh(\tilde{\omega}_{pq}t)). \tag{39}$$

Moreover, the latter case appears at most for a finite number of indices, and $\tilde{\omega}_{pq} < \frac{g_{pq}^2}{2}$.

Proof: We rewrite equation (34) as

$$\frac{d}{dt}U = \mathcal{A}U, \tag{40}$$

where $U = (u, u_t)$ and $\mathcal{A}$ is the following unbounded linear operator on $\mathcal{H}$:

$$\mathcal{A}(u, w) := (w, \psi_v * \Delta u - \varphi_h * w). \tag{41}$$

From (41) and (35), we deduce that

$$E_{pq} = \begin{pmatrix} 1 \\ \lambda_{\pm pq} \end{pmatrix} e_{pq} \tag{42}$$

are eigenvectors of $\mathcal{A}$ associated to the eigenvalues $\lambda_{\pm pq}$, solutions of

$$\lambda_{\pm pq}^2 + g_{pq}^2 \lambda_{\pm pq} + f_{pq}^2 (p^2 + q^2) = 0. \tag{43}$$

Moreover, the family of eigenvectors (E_{pq}) forms a Riesz basis of the Hilbert space $\mathcal{H}$. The discriminant of (43) is $\Delta_{pq} = g_{pq}^4 - 4(p^2+q^2)f_{pq}^2$. It can be positive for a finite number of indices only, since $g_{pq}^2 \to 0$ and $f_{pq}^2 \geq g\bar{h}$ when p and q go to infinity. We found a Riesz basis of $\mathcal{H}$ formed by eigenvectors of $\mathcal{A}$, the eigenvalues have no finite accumulation point and their real part are bounded. Thus all assumptions of theorem 3.1 of [14] are satisfied: the solution U of (40) is given by the series

$$\begin{aligned} U(t) = &\sum_{\substack{p,q\geq 1 \\ \Delta_{pq}<0}} \left(U_{pq} e^{\frac{-g_{pq}^2 + i\sqrt{4(p^2+q^2)f_{pq}^2 - g_{pq}^4}}{2} t} + U_{-pq} e^{\frac{-g_{pq}^2 - i\sqrt{4(p^2+q^2)f_{pq}^2 - g_{pq}^4}}{2} t} \right) E_{pq} \\ &+ \sum_{\substack{p,q\geq 1 \\ \Delta_{pq}\geq 0}} \left(U_{pq} e^{\frac{-g_{pq}^2 + \sqrt{g_{pq}^4 - 4(p^2+q^2)f_{pq}^2}}{2} t} + U_{-pq} e^{\frac{-g_{pq}^2 - \sqrt{g_{pq}^4 - 4(p^2+q^2)f_{pq}^2}}{2} t} \right) E_{pq}. \end{aligned} \tag{44}$$

Finally, the coefficients can be found using the Fourier series of the initial condition. We have

$$A_{pq} = \frac{4}{\pi^2} \int_{[0,\pi]^2} u(0,x,y) \sin(px) \sin(qy)\, dxdy, \tag{45}$$

$$B_{pq} = \frac{4}{\omega_{pq}\pi^2} \int_{[0,\pi]^2} \left(u_t(0,x,y) + \frac{g_{pq}^2}{2} u(0,x,y) \right) \sin(px) \sin(qy)\, dxdy \tag{46}$$

□

All we have to prove now is that the solution, which represents the estimation error, converges to 0 when time goes to infinity. Recall that the coefficients u_{pq} are given by equation (38), except for a finite number of indices. Define

$$u_N(t,x,y) = \frac{2}{\pi} \sum_{p+q\geq N} e^{\frac{-g_{pq}^2}{2} t} (A_{pq} \cos(\omega_{pq} t) + B_{pq} \sin(\omega_{pq} t)) \sin(px) \sin(qy). \tag{47}$$

Since $u_0 \in H_0^1(\Omega)$ and $u_1 \in L^2(\Omega)$, Parseval's theorem tells us that for any $\varepsilon > 0$, there exists N such that

$$\left\| u_N(t), \frac{\partial u_N}{\partial t}(t) \right\|_{\mathcal{H}} \leq \varepsilon/2, \quad \forall t \geq 0. \tag{48}$$

From (38) and (39), there exists $T > 0$ such that for any $t \geq T$,

$$\left\| (u - u_N)(t), \frac{\partial (u - u_N)}{\partial t}(t) \right\|_{\mathcal{H}} \leq \varepsilon/2. \tag{49}$$

Finally, $\|u, u_t\|_{\mathcal{H}} < \varepsilon$ for any $t \geq T$. We proved equation (32), i.e. the strong convergence of the linearized error system.

Note that this proves the result for any kernel functions defined by (27) and (28), provided all Fourier coefficients g_{pq}^2 are strictly positive. Note also that for $N > 0$ arbitrary large, from lemma 1, the truncated solution u_N tends to 0 exponentially in time. Thus exponential convergence is expected in numerical experiments.

3 Numerical simulations

In this section, we report the results of many numerical simulations on both the linearized and non-linear shallow water models, in order to illustrate the interest of such symmetry-preserving observers. The nonlinear observer is given by equations (18)-(19), with gain functions φ_h and φ_v given by equations (29)-(30). Although the gain design has been done on the simplified linearized system, the gains are also implemented on the non-linear observer (on the full non-linear shallow water model).

3.1 Linearized simplified system

We first consider a shallow water model, in a quasi-linear situation (small velocities, and height close to the equilibrium height) given by equations (16)-(17). The corresponding observer is solution of equations (18)-(19).

3.1.1 Model parameters

The numerical experiments are performed on a square box, of dimension 2000 km $\times$2000 km. The equilibrium height is $\bar{h} = 500$ m, and the equilibrium longitudinal and transversal velocities are $\bar{v}_x = \bar{v}_y = 0\ m.s^{-1}$. We consider a regular spatial discretization with 81×81 gridpoints. The corresponding space step is 25 km. The time step is half an hour (1800 seconds), and we have considered time periods of 1 to 4 months (1440 to 5760 time steps).

The reduced gravity is $g = 0.02\ m.s^{-2}$. The height varies between 497.7 and 501.9 m and the norm of the transversal velocity is within the interval $\pm 0.008\ m.s^{-1}$. The approximations of the preceding section are valid since $v \ll \sqrt{g\bar{h}} = 3\ m.s^{-1}$ and $\delta h \ll 500$. The variations of the height and velocities are indeed of the order of 2 meters and $0.01\, m.s^{-1}$ respectively. This kind of linearized system with the typical values above is often considered in geophysical applications, under the tangent linear approximation, for the estimation of an increment (instead of the solution itself) [5].

Concerning the tuning of the gains, we have considered the convolution kernels defined by equations (29)-(30). Recall that α_h^{-2} and α_v^{-2} represent the characteristic size of the Gaussian kernel. We will always take $\alpha_h^{-2} = \alpha_v^{-2} = \alpha$. In most of the experiments below we have $\alpha = 1\ m^{-2}$. Unfortunately the weights β_h and β_v cannot be chosen too large for numerical reasons, in order to

avoid stability issues. So we always take $\beta_h \leq 10^{-6}$. Recall that heuristically the error equation can be approximated by the damped wave equation (33) with $\bar{h}\beta_v = L_0^2\omega_0^2 - g\bar{h}$ and $\beta_h = 2\xi_0\omega_0$. The weights β_h and β_v have two different units, and physical meaning, and (a priori) there is no physical reason why they should have approximately the same magnitude. Nevertheless, for the numerical values of β_h considered in this paper, one can check that any value $0 \leq \beta_v \leq \beta_h$ yields a fundamental frequency for the error system $\omega_0\sqrt{1-\xi_0^2}$ which is close to the natural frequency $\sqrt{g\bar{h}}/L_0$ of the physical system (16)-(17). From now on we will systematically set $\beta_v = 0.1\ \beta_h$, which is acceptable from a physical point of view, also ensures the convergence of the observer, and is the largest value of β_v which yields numerical stability. Finally, a truncated convolution integral is used as an approximation of the complete convolution over the whole domain. The truncation radius is set equal to 10 pixels in our experiments (further than 10 pixels away from its center the Gaussian can be viewed as numerical noise).

We consider two criteria for quantifying the quality of the estimation process: the convergence rate of the estimation error, and the estimation error when convergence is reached. The initialization of the observer is always

$$\hat{h} = \bar{h}\ (= 500), \quad \hat{v} = \bar{v}\ (= 0).$$

In all the following results, the estimation error is the relative difference between the true solution (h and v) and the observer solution ($\hat{h}$ and $\hat{v}$):

$$e_h = \frac{\|(\hat{h}-\bar{h}) - (h-\bar{h})\|}{\|h-\bar{h}\|}, \qquad e_v = \frac{\|(\hat{v}-\bar{v}) - (v-\bar{v})\|}{\|v-\bar{v}\|} \tag{50}$$

where $\|\,.\,\|$ is the standard L^2 norm on the considered domain. With the previously defined initialization of the observer, the estimation error at initial time is $e_h(0) = e_v(0) = 1$, corresponding to a 100% error on the initial conditions. If we assume that the decrease rate is nearly constant in time, then the time evolution of the estimation error is given by:

$$e_h(t) = e_h(0)\exp(-c_h t), \qquad e_v(t) = e_v(0)\exp(-c_v t), \tag{51}$$

where c_h and c_v are the corresponding convergence rates. In all the numerical experiments that we have considered, the choice of the weighting coefficients β_h and β_v does not modify the residual estimation errors at convergence. One observes that the convergence rates are linearly proportional to β_h (and to $\beta_v = 0.1\beta_h$), provided it is not too large. This is explained by formula (37) as the Fourier coefficients g_{pq}^2 depend linearly on β_h.

3.1.2 Perfect observations

We first assume that the observations are perfect, i.e. without any noise. Figure 1 shows the estimation error (in relative norm) versus time (number of time steps), for the three variables: height h, longitudinal velocity v_x and transversal velocity v_y. The kernel coefficients are the following:

$$\beta_h = 5.10^{-7}\ s^{-1}, \quad \beta_v = 0.1\beta_h = 5.10^{-8}\ m.s^{-2}, \quad \alpha_h = \alpha_v = 1\ m^{-2}.$$

This figure shows that the convergence speed is nearly constant in time, and equation (51) is then valid. We can also deduce the corresponding convergence

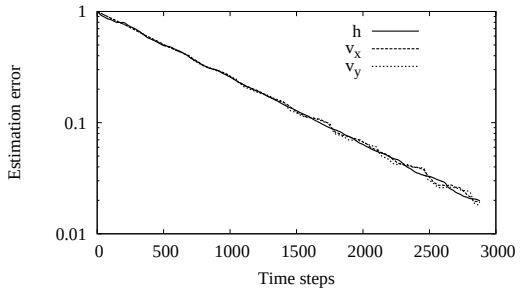

Figure 1: Evolution of the estimation error in relative norm versus the number of time steps, in the case of perfect observations, with $\alpha_h = \alpha_v = 1\ m^{-2}$ and $\beta_h = 5.10^{-7}\ s^{-1}$, and with a 100% error on the initial conditions, for the three variables: height h, longitudinal velocity v_x and transversal velocity v_y.

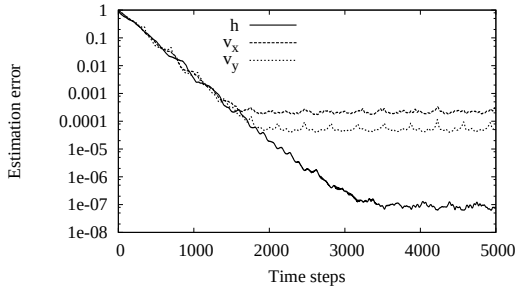

Figure 2: Evolution of the estimation error in relative norm versus the number of time steps, in the case of perfect observations, with $\alpha_h = \alpha_v = 1\ m^{-2}$ and $\beta_h = 2.10^{-6}\ s^{-1}$, for the three variables: height h, longitudinal velocity v_x and transversal velocity v_y.

rates:

$$c_h = 7.57 \times 10^{-7}, \qquad c_{v_x} = 7.63 \times 10^{-7}, \qquad c_{v_y} = 7.80 \times 10^{-7}.$$

Another interesting point is that, although only the variable h is observed, the velocity v is also corrected, with a comparable convergence rate. This is predicted by the theory above, but it is nevertheless extremely noticeable, as in most data assimilation processes, only a few variables of the system are observed [10, 23, 4]. This result shows (at least in the linear case) that all the variables are observable indeed.

Figure 2 shows the results of a similar experiment using different kernel coefficients ($\beta_h = 2.10^{-6}\ s^{-1}$, and still $\beta_v = 0.1\beta_h, \alpha_h = \alpha_v = 1\ m^{-2}$). The decrease rate is constant: $c_h = 2.84 \times 10^{-6}$, $c_{v_x} = 2.61 \times 10^{-6}$ and $c_{v_y} = 2.91 \times 10^{-6}$. The ratio between the decrease rate and β_h is almost preserved (the decrease rate has been multiplied by 3.5 to 3.75, and β_h by 4), as explained by formula (37). From now on, we will only give the decrease rate corresponding to the following weight values:

$$\beta_h = 5.10^{-7}\ s^{-1}, \qquad \beta_v = 0.1\beta_h = 5.10^{-8}\ m.s^{-2}.$$

Size of the gaussian kernel	Decrease rate $(h,\, v_x,\, v_y)$	Estimation error at convergence $(h,\, v_x,\, v_y)$
$\alpha_h = \alpha_v = 1$	7.58×10^{-7}	7.92×10^{-8}
	7.63×10^{-7}	2.11×10^{-4}
	7.80×10^{-7}	4.71×10^{-5}
$\alpha_h = \alpha_v = 10^3$	2.49×10^{-7}	1.02×10^{-7}
	2.61×10^{-7}	2.65×10^{-4}
	2.87×10^{-7}	6.12×10^{-5}

Table 1: Decrease rate and value at convergence of the estimation error, for the three variables h, v_x and v_y, for two different sizes of the gaussian kernel.

In both experiments, the estimation error at convergence has comparable (small) values:

$$e_h = 7.92 \times 10^{-8}, \qquad e_{v_x} = 2.11 \times 10^{-4}, \qquad e_{v_y} = 4.71 \times 10^{-5}.$$

From a theoretical point of view, it should converge to 0. Several reasons explain this difference with the theory. The numerical non-linear system considered is not exactly described by its first-order approximation. Moreover the numerical schemes and numerical noise do not allow the observer solution to reach exactly the observed trajectory. Note that the small oscillations in the decrease of the estimation error can be explained by the oscillatory behavior described by (37). Numerically speaking, the fact that the model has nearly no diffusion (no theoretical diffusion, and almost no numerical diffusion) can also contribute to this oscillatory phenomena.

Finally, we compare our observer to the standard nudging algorithm, by choosing a large value for α_h and α_v. Numerically we have set

$$\alpha_h = \alpha_v = 1000\ m^{-2}.$$

The decrease rate and estimation error at convergence are summarized in table 1 along with the previous results. The decrease rate of our observer is 2.7 to 3 times bigger. But assuming the solution (h, v) is constant (which is nearly true), the convolution with a gaussian kernel of size 1 or with a dirac produces the same effect, with a π factor (as $\int_{\mathbb{R}^2} e^{-(x^2+y^2)} dx\, dy = \pi$). Numerically, the factor is a little bit smaller, as the solution is not constant. We also see that the estimation error at convergence is a little bit larger for α large. Numerically, the small difference can probably be explained by some numerical noise, which is smoothed by the convolution.

3.1.3 Noisy observations

We now assume that the height h cannot be observed properly, and instead of h, we observe $h + \varepsilon$ where ε represents the observation noise on h. We assume that ε is gaussian with zero mean (white noise is standard in oceanography [9]), and a standard deviation of 20 to 40% of the standard deviation of the height h. Thus a 0.2 estimation error means that the estimated value $\hat{h}$ is closer to the true height h than to the observed height $h + \varepsilon$. Figure 3 shows similar experiments as previously described, in the case of noisy observations, for $\beta_h = 2.10^{-7}\ s^{-1}$

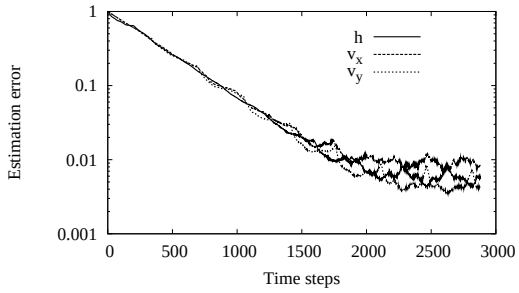

Figure 3: Evolution of the estimation error in relative norm versus the number of time steps, in the case of noisy observations (20% noise), with $\alpha_h = \alpha_v = 1\ m^{-2}$ and $\beta_h = 2.10^{-7}\ s^{-1}$, for the three variables: height h, longitudinal velocity v_x and transversal velocity v_y.

Size of the gaussian kernel	Decrease rate (h, v_x, v_y)	Estimation error at convergence (h, v_x, v_y)
$\alpha_h = \alpha_v = 0.5$	1.49×10^{-6}	4.43×10^{-3}
	1.40×10^{-6}	7.51×10^{-3}
	1.42×10^{-6}	4.06×10^{-3}
$\alpha_h = \alpha_v = 1$	7.55×10^{-7}	5.92×10^{-3}
	7.44×10^{-7}	1.04×10^{-2}
	7.44×10^{-7}	5.53×10^{-3}
$\alpha_h = \alpha_v = 10^3$	2.45×10^{-7}	1.70×10^{-2}
	2.49×10^{-7}	3.02×10^{-2}
	2.48×10^{-7}	1.59×10^{-2}

Table 2: Decrease rate and value at convergence of the estimation error, for the three variables h, v_x and v_y, for three different sizes of the gaussian kernel, in the case of noisy observations (20% noise).

and $\alpha = 1\ m^{-2}$. The global behaviour of the solution is unchanged (constant decrease until stabilization). The decrease rate and value at convergence of the estimation error for $\alpha = 0.5\ m^{-2}$, 1 and 10^3 are summarized in table 2.

There is still a ratio of nearly π between the decrease rate for α large and $\alpha = 1\ m^{-2}$. $\alpha = 0.5\ m^{-2}$ seems to be an optimal value for the parameter α: it is large enough to smooth efficiently the noise, and we checked that the decrease rate is not much larger when we take smaller values of α. Thus we see it is useless to correct the estimation at one point with values of h which are too far away from this point. In comparison with the case of perfect observations, the decrease rate is remarkably unaffected by the presence of noise.

The estimation error at convergence is much larger than in the case of perfect observations. Nevertheless, all variables have been identified with less than 1% of error. We see the interest of the convolution as the error at convergence is 3 to 4 times smaller with $\alpha \approx 1$ than with $\alpha = 1000$. This is due to the fact that the term $\nabla(\hat{h} - h)$ is very noisy when it is not directly filtered, as it is the case in the standard nudging algorithm (or extended Kalman filter).

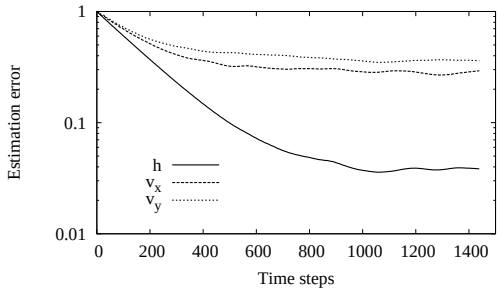

Figure 4: Evolution of the estimation error in relative norm versus the number of time steps, in the case of perfect observations, for $\beta_h = 5.10^{-7}\ s^{-1}$ and $\alpha_h = \alpha_v = 0.5\ m^{-2}$, for the three variables: height h, longitudinal velocity v_x and transversal velocity v_y.

3.2 Full nonlinear shallow water model

We now consider the full shallow water model, with the Coriolis force, friction, lateral viscosity, and wind stress (see equations (1)-(2)). We also consider large velocities and height variations, with still the same equilibrium point: $\bar{h} = 500$, $\bar{v}_x = \bar{v}_y = 0$. The size of the domain and the time and space steps remain the same as in the previous experiments (see section 3.1.1), the other physical parameters being:

$$f_0 = 7.10^{-5}s^{-1}, \quad \beta = 2.10^{-11}m^{-1}.s^{-1}, \quad R = 9.10^{-8}, \quad A = 5\,m^2.s^{-1}, \quad \tilde{\tau}_{max} = 0.05\,s^{-2}.$$

As we will see at the end of this section, this model reproduces quite well the evolution of a fluid in the northern hemisphere (e.g. Gulf Stream, in the case of the North Atlantic ocean, double-gyre circulation, ...), with realistic velocities and dimensions [19].

3.2.1 Perfect observations

We consider the same convolution kernels as in the experiments on the approximated system above, with the same reference parameters $\beta_h = 5.10^{-7}\ s^{-1}$ and $\beta_v = 0.1\beta_h$. Figure 4 shows the estimation error (in relative norm) versus time (number of time steps), for the three variables: h, v_x, v_y, with $\alpha_h = \alpha_v = 0.5\ m^{-2}$. Similar curves have been obtained with other values of α. The convergence speed for h, v are constant only at the beginning, and decrease continuously to 0 after the error goes under some treshold.

Table 3 summarizes the decrease rates at the beginning and the residual estimation error. The final estimation error is much larger than in the previous experiments. Consequently, if the velocity is not well retrieved, the height cannot be perfectly identified. Nevertheless the height estimation error is close to 1%, which is a very good result, considering the high turbulence of the model. The velocity is partially identified (with 12 to 15% of error in the best situations). The convergence rates are a little bit larger than in the linearized case. The behaviour between the standard gaussian convolution ($\alpha = 1\ m^{-2}$) and the Dirac convolution ($\alpha = 10^3\ m^{-2}$) is comparable to the previous experiments.

Size of the gaussian kernel	Decrease rate $(h,\, v_x,\, v_y)$	Estimation error at convergence $(h,\, v_x,\, v_y)$
$\alpha_h = \alpha_v = 0.5$	2.39×10^{-6}	3.73×10^{-2}
	1.79×10^{-6}	2.68×10^{-1}
	1.48×10^{-6}	3.47×10^{-1}
$\alpha_h = \alpha_v = 1$	1.29×10^{-6}	8.99×10^{-3}
	1.07×10^{-6}	1.24×10^{-1}
	8.58×10^{-7}	1.39×10^{-1}
$\alpha_h = \alpha_v = \times 10^3$	4.45×10^{-7}	1.46×10^{-2}
	3.19×10^{-7}	1.70×10^{-1}
	2.81×10^{-7}	2.16×10^{-1}

Table 3: Decrease rate and value at convergence of the estimation error, for the three variables h, v_x and v_y, for three different sizes of the gaussian kernel.

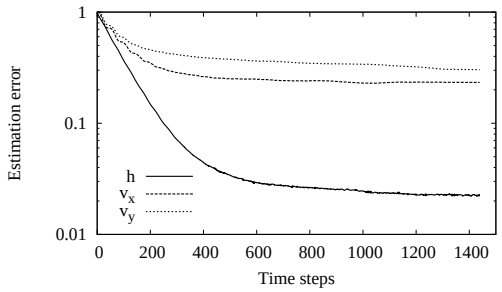

Figure 5: Evolution of the estimation error in relative norm versus the number of time steps, in the case of noisy observations (20% noise), for $\beta_h = 5.10^{-6}\ s^{-1}$ and $\alpha_h = \alpha_v = 10^3\ m^{-2}$, for the three variables: height h, longitudinal velocity v_x and transversal velocity v_y.

Note that the nonlinear model has a diffusion term, and hence regularizes much more the solution than the linearized model without diffusion. It explains why there are no oscillation as in the previous cases.

3.2.2 Noisy observations

As in the linearized situation, $h+\varepsilon$ is measured, where ε is assumed to be white. In our experiments, the standard deviation of ε is nearly 20% of the standard deviation of h (around the equilibrium state $\bar{h} = 500$).

The estimation error in the case of noisy observations is nearly 1.5 times larger than for perfect observations, both for $\alpha = 1\ m^{-2}$ and $\alpha = 10^3\ m^{-2}$. This confirms the relative insensitivity of the observer with respect to the presence of observation noise, as the level of noise is 20%, and the estimation errors are nearly 2% for h and 13 to 30% for the velocity. In this case, the best results have been obtained for $\alpha = 1\ m^{-2}$, improving the results of the nudging algorithm ($\alpha = 10^3\ m^{-2}$) of 33 to 50%. These results clearly show the interest of a gaussian kernel applied to the correction term, in order to smooth the noisy observations (or the numerical noise).

Size of the gaussian kernel	Decrease rate $(h,\, v_x,\, v_y)$	Estimation error at convergence $(h,\, v_x,\, v_y)$
$\alpha_h = \alpha_v = 0.5$	2.74×10^{-6} 1.87×10^{-6} 1.62×10^{-6}	1.71×10^{-2} 1.72×10^{-1} 2.21×10^{-1}
$\alpha_h = \alpha_v = 1$	1.36×10^{-6} 9.65×10^{-7} 8.38×10^{-7}	1.57×10^{-2} 1.30×10^{-1} 1.59×10^{-1}
$\alpha_h = \alpha_v = 10^3$	4.42×10^{-7} 2.98×10^{-7} 2.55×10^{-7}	2.26×10^{-2} 2.25×10^{-1} 3.04×10^{-1}

Table 4: Decrease rate and value at convergence of the estimation error, for the three variables h, v_x and v_y, for three different sizes of the gaussian kernel, in the case of noisy observations (20% noise).

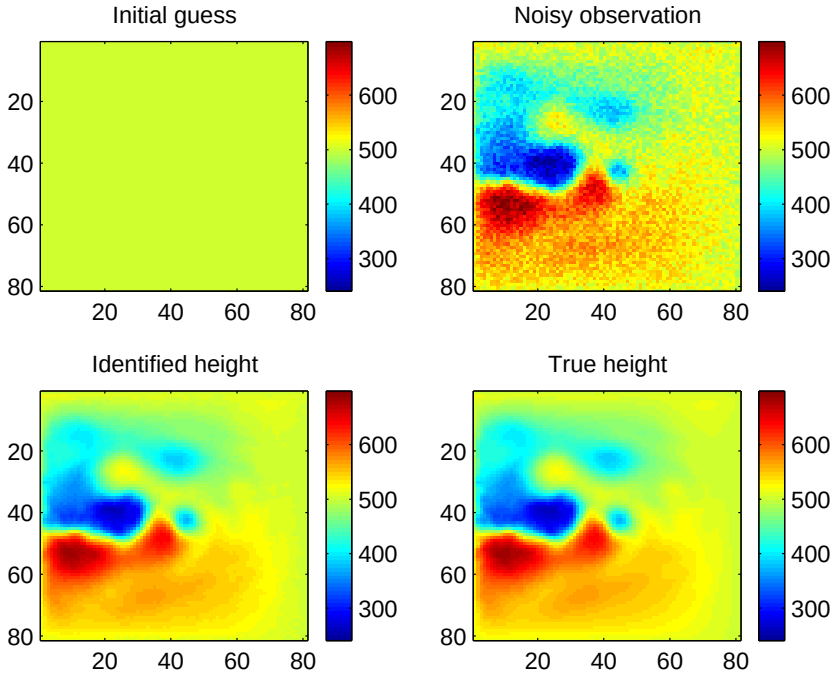

Figure 6: Identification process for the height, in meters: initial guess ($\hat{h}(0) = \bar{h}$); noisy observation at final time ($h(T) + \varepsilon$, with $T = 1440$ time steps); identified height at final time ($\hat{h}(T)$); true height at final time ($h(T)$).

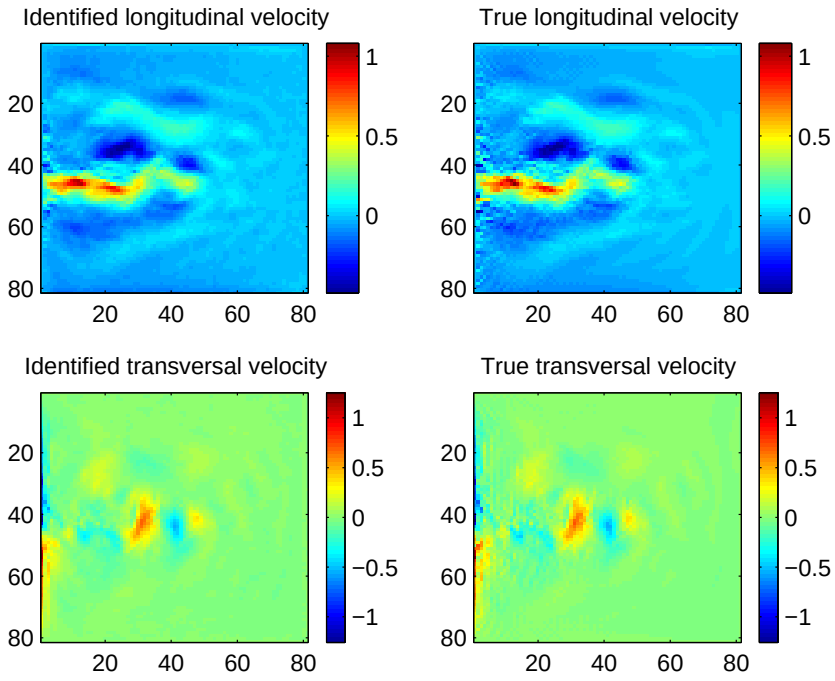

Figure 7: Identification process for the velocity, in $m.s^{-1}$: identified longitudinal (resp. transversal) velocity at final time ($\hat{v}(T)$); true longitudinal (resp. transversal) velocity at final time ($v(T)$).

Finally, figures 6 and 7 illustrate the identification process for both the height and velocity in the case of noisy observations, for $\alpha_h = \alpha_v = 1$ (second case of table 4). We do not use any a priori information, as the initial guess is $\hat{h} = \bar{h} = 500$ meters (top left image of figure 6), and $\hat{v} = \bar{v} = 0\ m.s^{-1}$. Figure 6 shows on the top right the noisy observation $h + \varepsilon$ of the height at the final time $T = 1400$ time steps. It should be compared to the bottom right image, showing the true height h at the same time. The difference between these two images corresponds to the white Gaussian noise ε. Finally, the identified height (i.e. the observer $\hat{h}$ at final time T) is shown on the bottom left image of figure 6. These images confirm both the very good identification of the height (as previously seen in table 4) and the noise removal.

Figure 7 shows the identified and real components of the velocity. Note that even if there are no observations of the velocity, the observer $\hat{v}$ is very close to the real velocity v at time T. This is usually not the case in standard nudging techniques, where only observed variables are corrected [10, 23, 4]. The main current (correponding to the Gulf Stream, in the case of the North Atlantic ocean) is very well identified. This is extremely interesting, as in real geophysical applications, there are also almost no observations of the fluid velocity, although it has to be identified precisely [5]. From table 4, we have previously seen that the error on the velocity is nearly 15% in this case, which is quite high. But the main currents are very well identified, and this is a key-point for improving the quality of the forecasts. In most geophysical data assimilation problems, the non-observed variables are only corrected thanks to model coupling, and it does not lead to such a nice identification [13].

4 Conclusion

In this paper, we have defined a class of symmetry-preserving observers for a simplified and linearized shallow water model. We proved the convergence to zero of the error (i.e. difference between the observer and real trajectories) when time goes to infinity. Many numerical simulations show the interest of such a choice of invariant gains. This paper gives insight in the field of non-linear observers for infinite dimensional systems, where very few methods are available.

The observer provides better results than the standard nudging, even on the nonlinear system, as the error converges faster, the residual error is smaller, and the observer is much more robust to noise. The correction terms used in this paper are different from those of the usual extended Kalman filter-type estimators (no integral over space is performed). Our observer has several advantages upon the extended Kalman filter. First the computation cost is much smaller (as long as the gaussian kernel is set equal to zero wherever its value is negligible, see Section 3). This is important as in oceanographic data assimilation, the computation cost of the Kalman filter can be prohibitive, as well as the cost of optimal nudging techniques [24]. Moreover the tuning of the gains of our observer is very easy as they depend on a very reduced number of parameters which have a physical meaning. It is precisely the use of the physical structure of the system which allows us to reduce the degrees of freedom in the gain design. Finally, to the author's knowledge, there is no proof of convergence of the Kalman filter for infinite dimensional non-linear systems. Note that we also showed, both on

theoretical and numerical points of view, that thanks to an appropriate choice of observer, it is possible to correct very well the non-observed variables with the observed ones, which is still a challenge in oceanography (and more generally in geophysics) [5].

Other types of correction terms could be used. In particular one could define the correction term in order to get the following linearized error equation instead of (26):

$$\frac{\partial^2}{\partial t^2}\tilde{h} = (g\bar{h}\delta_0 + \varphi_v) * \Delta\tilde{h} - \varphi_h * \frac{\partial}{\partial t}\tilde{h} + \varphi_h^{\Delta} * \Delta\left(\frac{\partial}{\partial t}\tilde{h}\right). \tag{52}$$

Indeed an additional structural damping would drastically change the spectrum. The use of such terms is generally prohibited by the presence of measurement noise, but the convolution product with a smooth kernel would allow us to use them. Another direction for future work would be to make numerical experiments on back and forth nudging based on our observer. The observer can easily be adapted in reverse time indeed, with $\varphi_h \mapsto -\varphi_h$ and φ_v unchanged (see e.g. [4] for details about this data assimilation method). Finally, in this paper we only considered time and space continuous measurements. Some experiments will also be carried out in the case of sparse observations, both in time and space. As a more general concluding remark, although this paper is only concerned with examples, it shows a systematical way to take advantage of the rotational invariance of the Laplacian, and yields a method for the convergence analysis. This technique could be adapted to other estimation problems from physics and engineering, where the models are based on the wave equation or on the heat equation.

Aknowledgements

This paper is supported by the CNRS. The authors would like to warmly thank all members of the LEFE BFN project for useful discussions.

References

[1] N. Aghannan and P. Rouchon. On invariant asymptotic observers. In *Proc. of the 41st IEEE Conf. on Decision and Control*, volume 2, pages 1479–1484, 2002.

[2] N. Aghannan and P. Rouchon. An intrinsic observer for a class of lagrangian systems. *IEEE Trans. Autom. Contr.*, 48(6):936–945, 2003.

[3] L. Alvarez, F. Guichard, P.-L. Lions, and J.-M. Morel. Axioms and fundamental equations of image processing. *Arch. Rational Mech. Anal.*, 123:199–257, 1993.

[4] D. Auroux and J. Blum. A nudging-based data assimilation method for oceanographic problems: the Back and Forth Nudging (BFN) algorithm. *Nonlin. Proc. Geophys.*, 15:305–319, 2008.

[5] A. F. Bennett. *Inverse Modeling of the Ocean and Atmosphere*. Cambridge University Press, Cambridge, 2002.

[6] S. Bonnabel, Ph. Martin, and P. Rouchon. Non-linear symmetry-preserving observers on lie groups. *IEEE Trans. Autom. Contr.*, 2008. Accepted for publication.

[7] S. Bonnabel, Ph. Martin, and P. Rouchon. Symmetry-preserving observers. *IEEE Trans. Automat. Contr.*, 2008. In press.

[8] F. Dubois, N. Petit, and P. Rouchon. Motion planing and nonlinear simulations for a tank containing a fluid. In *European Control Conference, Karlsruhe*, 1999.

[9] G. Evensen. The ensemble Kalman filter: Theoretical formulation and practical implementation. *Ocean Dynam.*, 53:343–367, 2003.

[10] J. Hoke and R. A. Anthes. The initialization of numerical models by a dynamic initialization technique. *Month. Weather Rev.*, 104:1551–1556, 1976.

[11] S. Jiang and M. Ghil. Tracking nonlinear solutions with simulated altimetric data in a shallow-water model. *J. Phys. Oceanogr.*, 27(1):72–95, 1997.

[12] R. E. Kalman. A new approach to linear filtering and prediction problems. *Trans. ASME - J. Basic Engin.*, 82:35–45, 1960.

[13] E. Kalnay. *Atmospheric modeling, data assimilation and predictability.* Cambridge University Press, 2003.

[14] V. Komornik and P. Loreti. *Fourier Series in Control Theory.* Springer Monographs in Mathematics. Springer-Verlag, New York, 2005.

[15] F.-X. Le Dimet and O. Talagrand. Variational algorithms for analysis and assimilation of meteorological observations: theoretical aspects. *Tellus*, 38A:97–110, 1986.

[16] D. Luenberger. Observers for multivariable systems. *IEEE Trans. Autom. Contr.*, 11:190–197, 1966.

[17] R. Mahony, T. Hamel, and J.-M. Pflimlin. Complimentary filter design on the special orthogonal group SO(3). In *Proc. IEEE Conf. on Decision and Control, CDC05, Seville*, 2005.

[18] P. J. Olver. *Equivalence, Invariants, and Symmetry.* Cambridge University Press, 1995.

[19] J. Pedlosky. *Geophysical fluid dynamics.* Springer-Verlag, New-York, 1979.

[20] N. Petit and P. Rouchon. Dynamics and solutions to some control problems for water-tank systems. *IEEE Trans. Automat. Contr.*, 47(4):594–609, 2002.

[21] D. Rozier, F. Birol, E. Cosme, P. Brasseur, J.-M. Brankart, and J. Verron. A reduced-order Kalman filter for data assimilation in physical oceanography. *SIAM Rev.*, 49(3):449–465, 2007.

[22] L. Schwartz. Opérateurs invariants par rotations. Fonctions métaharmoniques. In *Séminaire Schwartz*, volume 2(9), pages 1–5, 1954.

[23] J. Verron and W. R. Holland. Impact de données d'altimétrie satellitaire sur les simulations numériques des circulations générales océaniques aux latitudes moyennes. *Annales Geophysicae*, 7(1):31–46, 1989.

[24] X. Zou, I. M. Navon, and F.-X. Le Dimet. An optimal nudging data assimilation scheme using parameter estimation. *Q. J. R. Meteorol. Soc.*, 118:1163–1186, 1992.

Centre de recherche INRIA Grenoble – Rhône-Alpes
655, avenue de l'Europe - 38334 Montbonnot Saint-Ismier (France)

Centre de recherche INRIA Bordeaux – Sud Ouest : Domaine Universitaire - 351, cours de la Libération - 33405 Talence Cedex
Centre de recherche INRIA Lille – Nord Europe : Parc Scientifique de la Haute Borne - 40, avenue Halley - 59650 Villeneuve d'Ascq
Centre de recherche INRIA Nancy – Grand Est : LORIA, Technopôle de Nancy-Brabois - Campus scientifique
615, rue du Jardin Botanique - BP 101 - 54602 Villers-lès-Nancy Cedex
Centre de recherche INRIA Paris – Rocquencourt : Domaine de Voluceau - Rocquencourt - BP 105 - 78153 Le Chesnay Cedex
Centre de recherche INRIA Rennes – Bretagne Atlantique : IRISA, Campus universitaire de Beaulieu - 35042 Rennes Cedex
Centre de recherche INRIA Saclay – Île-de-France : Parc Orsay Université - ZAC des Vignes : 4, rue Jacques Monod - 91893 Orsay Cedex
Centre de recherche INRIA Sophia Antipolis – Méditerranée : 2004, route des Lucioles - BP 93 - 06902 Sophia Antipolis Cedex

Éditeur
INRIA - Domaine de Voluceau - Rocquencourt, BP 105 - 78153 Le Chesnay Cedex (France)
http://www.inria.fr
ISSN 0249-6399